

# TrustGeoGen: Formal-Verified Data Engine for Trustworthy Multi-modal Geometric Problem Solving

Daocheng Fu, Jianlong Chen, Renqiu Xia, Zijun Chen, Qi Liu, Yuan Feng, Hongbin Zhou, Renrui Zhang, Shiyang Feng, Peng Gao, Hongyuan Zha, Junchi Yan, Botian Shi, Yu Qiao, Bo Zhang

**Abstract**—Mathematical geometric problem solving (GPS) demands verifiable logical coherence and multimodal reasoning capabilities. While large language models (LLMs) have shown rapid progress in GPS, their advancement is hindered by the lack of reliable benchmarks and systematic methodologies. A critical challenge is the inherent hallucination in LLMs, which leads to synthetic GPS datasets that are often noisy, unverified, and self-contradictory. To address this, we introduce TrustGeoGen, a data engine that generates formally verified geometric problems to establish a principled and trustworthy benchmark. Our engine integrates four key innovations: 1) Multimodal Alignment, which synchronizes the generation of diagrams, text, and step-by-step solutions; 2) Formal Verification, ensuring all reasoning paths are rule-compliant; 3) Connection Thinking, bridging formal deduction with human-like logical steps; and 4) our *GeoExplore* series algorithms, which produce diverse problem variants with multiple solutions and self-reflective backtracking. Using this engine, we create the GeoTrust-200K dataset and the corresponding GeoTrust-test benchmark, both with guaranteed cross-modal integrity. Experiments reveal that state-of-the-art models achieve only 45.83% accuracy on GeoTrust-test, highlighting its significant challenge. Furthermore, training on our synthesized data substantially improves model performance on GPS tasks, with strong generalization to out-of-domain (OOD) benchmarks. Our code and data are available at <https://github.com/Alpha-Innovator/TrustGeoGen>.

**Index Terms**—Data Engine, Geometry, Multi-modal



## 1 INTRODUCTION

GEOMETRIC problem solving (GPS) [44], as a pivotal branch of mathematical reasoning or more broadly speaking, general reasoning, demands tripartite capabilities: 1) extracting spatial relationships from visual diagrams, 2) performing mathematical reasoning in language modality, and 3) maintaining stepwise logical coherence where intermediate conclusions rigorously justify subsequent deductions. The development of trustworthy AGI systems fundamentally relies on reliably annotated multimodal data that not only bridges visual-textual modalities but also preserves closed-loop reasoning chains. This requirement stems from a critical axiom: a geometrically valid solution demands both correct answers and air-tight logical pathways, as human experts reject proofs with *leap-of-faith*<sup>1</sup> arguments even when final results are accurate.

The recent advancement of multimodal large language models (MLLMs) [4, 10, 14, 15, 17, 26, 27, 30, 33, 35, 43, 44] has revealed promising capabilities in geometric reasoning, demonstrating competence in solving elementary geometric problems. Parallel developments in external formalized expert systems [8, 24, 28, 51] have extended problem solving capabilities to more complex geometric configurations, with highly specialized models [11, 41, 49] even approaching challenges of the international mathematical olympiad (IMO) level. However, these achievements are critically dependent on high-quality geometric data, currently in short supply. The existing datasets are mainly derived from manual annotations of secondary school textbook problems [8, 9, 19, 28, 51], and this process is limited in scale and diversity. Although recent integration of MLLMs (e.g. GPT series [1, 29, 30]) for synthetic question-answer generation [17, 53] has partially ameliorated data scarcity concerns, significant challenges persist in ensuring *stepwise solution validity*<sup>2</sup>, which may undermine the logical coherence of reasoning chains during model training.

However, as depicted in table 1, current geometric datasets exhibit four deficiencies: **1) Modality Fragmentation:** The existing datasets suffer from incomplete modality alignment, lacking annotations that synchronize images, textual captions, questions, and chain-of-thought reasoning processes within unified instances. **2) Scalability Issues:**

- Daocheng Fu, Jianlong Chen, Renqiu Xia and Zijun Chen contribute equally to this work.
- Corresponding authors: Bo Zhang (E-mail: zhangbo@pjlab.org.cn) and Renqiu Xia (E-mail: xiarenqiu@sjtu.edu.cn).
- Daocheng Fu is with College of Computer Science and Artificial Intelligence, Fudan University.
- Daocheng Fu, Hongbin Zhou, Renrui Zhang, Shiyang Feng, Peng Gao, Botian Shi, Yu Qiao and Bo Zhang are with Shanghai Artificial Intelligence Laboratory, Shanghai 200232, China.
- Jianlong Chen and Hongyuan Zha are with The Chinese University of Hong Kong, Shenzhen.
- Renqiu Xia, Zijun Chen, Qi Liu, Yuan Feng and Junchi Yan are School of Artificial Intelligence, Shanghai Jiao Tong University.

1. Here it means an unjustified or unsubstantiated jump in reasoning, where a conclusion is reached with insufficient logical steps or evidence.

2. Specifically, automatically generated procedural labels frequently contain latent inconsistencies, such as misapplied geometric axioms or diagram-coordinate mismatches.

TABLE 1: Comparison of various geometric problem-solving datasets and benchmarks. Modality abbreviations: I for Image, FS for Formal Solution, NS for Natural Solution, A for Answer. Thinking Template abbreviations: D for Deductive, BT for Backtrack, MS for Multi-solution.

Datasets & Benchmarks	Size	Modality	Level	Thinking Template	Labeling Method
GeoQA [9]	4998	I, NS, A	Middle School	D	Human Annotation
GeoQA+ [7]	7528	I, NS, A	Middle School	D	Human Annotation
Geometry3K [28]	3002	I, FS, A	Middle School	D	Step-wise Formal Verified
PGPS9K [51]	9022	I, FS, A	Middle School	D	Step-wise Formal Verified
UniGeo [8]	9543	I, NS, A	Middle School	D	From Source File
GeoEval [50]	5050	I, A	Middle & High School	-	LLM Labeling
MathVista [27]	1320 *	I, A	Middle School	-	From Source File
MathVerse [52]	1745 *	I, NS, A	High School	-	LLM Labeling
GeoSense [22]	1789	I, NS, A	Synthetic	D	LLM Labeling & Human Annotation
OlympiadBench [20]	8476	I, NS, A	Olympiad-level	D	From Source File
MAVIS [53]	588K	I, NS, A	Synthetic	D	LLM Labeling
G-LLAVA [17]	170K	I, NS, A	Synthetic	D	LLM Labeling
TrustGeoGen	200K	I, FS, NS, A	Synthetic	D, MS, BT	Step-wise Formal Verified
GeoTrust-train	2342	I, FS, NS, A	Synthetic	D, MS, BT	Step-wise Formal Verified
GeoTrust-test	240	I, FS, NS, A	Synthetic	D	Step-wise Formal Verified

\* These values are not the total count but the count of the GPS category within the dataset.

Most approaches rely on repurposing human-authored problems from textbooks or examinations rather than generating novel, curriculum-aligned challenges. **3) Cost Constraints:** Manual annotation requires costly geometry expertise, while generating solutions through MLLMs consumes excessive computational resources. **4) Trust Deficits:** Model-generated solutions lack reliable automated verification mechanisms, introducing risks of undetected logical errors or misaligned reasoning steps.

To this end, we develop **TrustGeoGen**, a formal language-verified geometric data generation engine that autonomously produces geometric problems, diagrams, and stepwise solutions through four integrated components: 1) a *Constructor* to generate constraint-satisfying problem premises and diagrams, 2) a *Reasoner* expanding geometrically valid reasoning graphs with rigorous node verification, 3) a *Sampler* leveraging the algorithm *GeoExplore* to extract high-quality reasoning paths, which are later converted into problems by pairing initial premises with derived conclusions, and 4) A *Translator* converting the data constructed by the formal engine into natural language, and establishing "connection thinking" to bridge the gap between formal reasoning steps and natural human logic. Furthermore, we improve the problem complexity through a bootstrapping mechanism in TrustGeoGen, where formally verified geometric premises in prior stages are recursively fed back to the *Constructor* to iteratively append new premises. This closed-loop process enables systematic escalation of difficulties while maintaining logical consistency. Additionally, we refine the algorithm *GeoExplore* to simultaneously explore alternative solution paths and self-correcting reasoning trajectories, generating problems with multiple valid solutions and self-reflective traceback data.

Our proposed TrustGeoGen ensures: 1) **Modality Completeness** with synchronized dual-form (formal & informal) captions, questions, solutions, and diagrams, 2) **Scalability** in generating geometry problems by bootstrapping mechanisms without reliance on existing data source and 3) **Verifiability** through formal validation of all solution steps in its integrated reasoner. Leveraging TrustGeoGen,

we synthesized a raw dataset of 200K problems, from which we curated the *GeoTrust-train* set (2,342 samples) and the *GeoTrust-test* set (240 samples).

Our experimental results demonstrate that the data generated by TrustGeoGen not only reaches a difficulty level comparable to the international mathematical olympiad (IMO) but also contains novel problems unseen in the pre-training corpora of state-of-the-art (SOTA) models, thereby enhancing their performance. Furthermore, the "connection thinking" provided by the translator bridges the gap between formal engine-verified reasoning paths and human-like logical inference, significantly boosting the model's geometric problem-solving abilities. The data constructed from "thinking templates" by the *GeoExplore* series of algorithms has also been proven effective in improving the model's reasoning capabilities. Additionally, our training data from GeoTrust enhances model performance on the out-of-distribution (OOD) testset GeoQA [9], Geometry3K [28], and OlympiadBench [20], highlighting its broader generalization capability. The main contributions of this paper can be summarized as follow:

- We develop **TrustGeoGen**, a formalized geometric data generation engine, producing multimodal-integrated data (geometric diagrams, formal & natural language captions, questions and solutions) with trustworthy reasoning guarantees via formal verification.
- We introduce "Connection Thinking" to bridge the gap between formal and human-like logical reasoning, enabling our engine to enhance models' reasoning capabilities. Our *GeoExplore* series algorithms further synthesize data with diverse thinking templates, offering different problem-solving pathways.
- Extensive experiments show that **TrustGeoGen** generates challenging, verifiable data that significantly improves models' geometric problem-solving abilities. Results on OOD datasets demonstrate the effectiveness and generalization of our synthetic data.



often exists between the synthesized logic and authentic human reasoning, leaving considerable room for improvement in enhancing the model's natural language inference abilities. Finally, the third method employs LLMs to synthesize reasoning data [17, 53]. This method is highly efficient, and the generated reasoning steps more closely resemble natural language. Its primary drawback, however, is that the outputs are unverifiable; they may contain erroneous intermediate steps that could mislead or corrupt the model's reasoning capabilities.

### 3 METHODOLOGY

The data engine TrustGeoGen serves as the core for constructing high-quality geometric reasoning datasets, enabling the generation of complex geometric scenes and reasoning paths to support robust and scalable inference.

#### 3.1 Data Engine

In the process of generating multi-modal geometric reasoning data, it employs a rule-based data construction method augmented by a geometric verifier to synthesize high-quality datasets. This approach ensures that the generated data are accurate and controllable. As shown in fig. 1, our framework consists of four components: Constructor, Reasoner, Sampler, and Translator.

**Constructor** is responsible for generating a geometric scene for a given problem. The foundational components of this process are constructions ( $C$ ) and statements ( $s$ ). A geometric scene is described by a sequence of constructions, where each construction  $C_i$  generates one or more statements, such as  $\{s_i^1, s_i^2, \dots\}$ , that define the relationships between geometric elements. Before a new construction can be added to the scene, the existing statements must satisfy its preconditions. For instance, to apply the construction "draw a perpendicular from point  $A$  to line  $BC$ , with  $D$  as the foot," the precondition "points  $A$ ,  $B$ , and  $C$  are not collinear" must hold true. Conversely, the successful application of a construction yields new statements. For example, the construction "create an isosceles triangle  $ABC$ " introduces the statements " $AB = AC$ " and " $\angle ABC = \angle ACB$ ". Following this paradigm, a complete geometric scene, described by  $\{C_1, C_2, \dots, C_n\}$ , can be built incrementally from scratch. This process concurrently generates the scene's definitive set of initial statements,  $S_0 = \{s_1^1, s_1^2, \dots, s_n^1, s_n^2, \dots\}$ , which is the total collection of all generated statements.

To ensure the generated scenes are both geometrically significant and numerically instantiated, we have hand-crafted a library of 46 base scene generation functions. These functions produce primitive geometric configurations populated with random numerical values. As shown in fig. 1, the **Constructor** initiates the process by randomly selecting one of these functions to create an initial, numerically-defined scene. Subsequently, it iteratively adds further constructions, contingent on their preconditions being met, until a target scene is fully formed. This scene is then passed to a geometric compiler for validation, which checks for the consistency of all geometric relations and constraints. Ultimately, once a valid geometric scene is successfully constructed, its complete set of initial statements,  $S_0$ , can be obtained.

---

#### Algorithm 1: GeoExplore

---

**Require:** Reasoning graph  $\mathcal{G} = (S, S_0, R, \hookrightarrow)$ , target statement  $s_n$ , threshold  $\tau_l$ , threshold  $\tau_r$

**Ensure:** Filtered reasoning path  $\mathcal{P}$

```

1 Initialize  $\mathcal{P} \leftarrow \emptyset$ ;
2  $s \leftarrow s_n$ ;
3 while  $s \notin S_0$  do
4   Identify rule  $r_s \in R$  and parent statement set
      $S_{i-1} \subset S$  such that  $S_{i-1} \xrightarrow{r_s} s$ ;
5   Append transition  $(S_{i-1}, r_s, s)$  to  $\mathcal{P}$ ;
6    $s \leftarrow S_{i-1}$ ;
7 Assess path length:  $L \leftarrow |\mathcal{P}|$ ;
8 Compute premises ratio:  $R_P \leftarrow |S_P|/|S_0|$ , where
    $S_P \subseteq \mathcal{P}$ ;
9 if  $L \geq \tau_l$  and  $R_P \geq \tau_r$  then
10  return  $\mathcal{P}$ ;
11 else
12  Discard  $\mathcal{P}$ ;

```

---

**Reasoner** leverages a predefined set of geometric theorems to infer new statements from premises generated by the *constructor*, formulating a reasoning graph:

$$\mathcal{G} = (S, S_0, R, \hookrightarrow), \quad (1)$$

- $S$  is the set of statements, where each statement  $s \in S$  represents a derived conclusion or fact in the reasoning process.
- $S_0 \subseteq S$  is the set of initial statements generated by the *constructor*.
- $R$  is the set of rules, where each rule  $r \in R$  defines a logical inference relationship between statements.
- $\hookrightarrow \subseteq S \times R \times S = \{(S_r, r, s') \mid S_r \subset S, r \in R, s' \in S\}$  is the statement transition relation. A transition  $S_r \xrightarrow{r} s'$  indicates statement  $s'$  is derived from  $s$  by applying rule  $r$ .

Reasoning begins with the initial statement  $S_0$  (given premises from the **constructor**), forming the root nodes of the graph  $\mathcal{G}$ . The graph expands by applying inference rules to existing statements. For every statement set  $S_r \subset S$  and rule  $r \in R$ , if  $r$  can be applied to  $S_r$  to derive a new statement  $s'$  (formally  $S_r \xrightarrow{r} s'$ ), the reasoner performs two atomic updates: 1) Add the new statement  $S_r$  to  $S$  and 2) Add the edges  $(S_r, s')$  to the transition relation  $\hookrightarrow$  with rule  $r$ . Finally, the complete graph is the smallest closure satisfying:

$$S = S_0 \cup \{s' \mid \forall S_r \subset S, r \in R, S_r \xrightarrow{r} s'\}. \quad (2)$$

**Sampler** operates on the reasoning graph  $\mathcal{G}$  by sampling a target statement  $s_n$  and subsequently searching for its path:

$$\mathcal{P} = \{(S_{i-1}, r_s, s) \mid \forall s \in S, S_{i-1} \xrightarrow{r_s} s, i = n, \dots, 1\}, \quad (3)$$

where each triplet  $(S_i, r_s, s)$  denotes a specific transition during the reasoning process, derived by applying rule  $r_s$  to statement set  $S_{i-1}$  to produce statement  $s$ . Any statement  $s_n$  within the statement set  $S$  can be treated as a problem to solve in order to derive a reasoning path  $\mathcal{P}$ . The sampler



is initialized with a statement  $s \in S_n$  to retrieve the corresponding transition rule  $r_s$  and the upstream dependent statements  $S_i$ . This process is repeated iteratively until the statement set  $S_i$  consists entirely of initial premises  $S_0$ . At that point, the full reasoning path has been successfully constructed. Notably, during the graph construction process in the **Reasoner**, once a statement  $s$  is derived through rule  $r_s$ , no additional statement transition relations are appended to  $s$ . Consequently, the **Sampler** is always able to identify a unique inference rule  $r_s$  corresponding to any statement  $s$ , thereby guaranteeing the absence of cycles in the reasoning path.

To ensure the quality of the reasoning paths, the **Sampler** employs two metrics to filter out unsuitable paths. The first metric evaluates the length of the reasoning path  $\mathcal{P}$  against a predefined threshold  $\tau_l$ . If the length of  $\mathcal{P}$  exceeds  $\tau_l$ , the path is considered difficult enough. Formally, this condition is expressed as  $|\mathcal{P}| \geq \tau_l$ , where  $|\mathcal{P}|$  denotes the number of transitions in the reasoning path  $\mathcal{P}$ . The second metric assesses the ratio of the statements in the reasoning path  $\mathcal{P}$  that are derived from the initial premises set  $S_0$ . If this ratio exceeds a predefined threshold  $\tau_r$ , the path is deemed sufficient enough. This condition is formally defined as  $\frac{|S_P|}{|S_0|} \geq \tau_r$ , where  $|S_P|$  represents the number of initial premises used in the reasoning path  $\mathcal{P}$ , and  $|S_0|$  is the number of all initial premises. By applying these two metrics, the **Sampler** ensures that only high-quality reasoning paths are retained, thereby maintaining the integrity and usefulness of the generated data. The detailed procedure of the aforementioned reasoning path exploration and filtering algorithm, *GeoExplore*, is presented in algorithm 1.

**Translator** is tasked with converting the reasoning steps synthesized by a formal engine into natural language narratives. These narratives serve as high-quality training data to cultivate the reasoning capabilities of Large Language Models (LLMs). As illustrated in fig. 2, the Translator's process is twofold. First, it employs a state-of-the-art LLM (GPT-4o) to translate each formal reasoning step into its natural language counterpart. Given the highly structured format of the formal steps, we utilize a few-shot prompting strategy. This approach facilitates a step-by-step translation process rather than a single-pass generation of the entire sequence, thereby significantly enhancing translation fidelity.

However, a direct translation, while lexically aligned with human language, still mirrors the discrete, logical leaps of the formal engine, differing substantially from human cognitive processes. A key limitation is the absence of explicit logical bridges between consecutive steps, failing to articulate how one deduction leads to the next. Training an LLM on such data risks encouraging it to overfit to the syntactic structure of the formal expressions, rather than internalizing the underlying reasoning process. To mitigate this, the Translator executes a second crucial task: interleaving bridging rationales. It uses the translated steps as a scaffold and prompts GPT-4o to articulate the intermediate thought process. Specifically, for each step, the model first summarizes the currently established facts, then explicates how these facts logically connect to the subsequent step, and how this progression contributes to reaching the final goal. This method of generating explicit "Connection Thinking" compels the model to engage in a deeper level of infer-

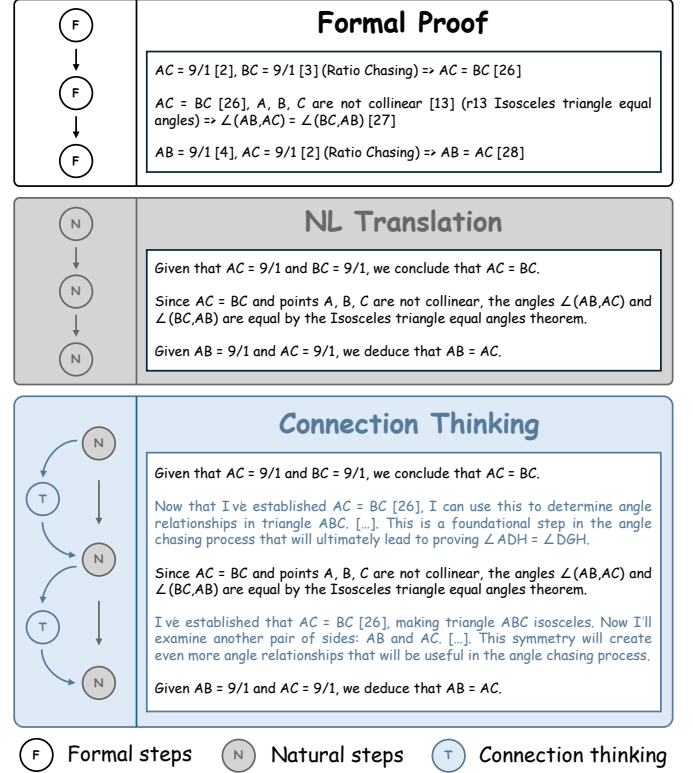


Fig. 2: Simple illustration of how Translator works

ence, ultimately enhancing the reasoning performance of the models trained on this data.

### 3.2 Bootstrap Augmentation

As previously described, TrustGeoGen begins by constructing a complex geometric figure from a completely random initial scenario and then derives reasoning paths for this instance. While this approach is scalable, its efficiency in generating high-quality data is relatively low, as it may randomly produce geometric scenarios that fail to yield meaningful or valuable results. To address this, TrustGeoGen employs an iterative bootstrap strategy to guide the generation process, thereby improving the efficiency of producing high-quality data. In each iteration, TrustGeoGen utilizes the metrics from the Sampler to evaluate the quality of sampled data on a given graph  $G$ . If the average quality of the sampled data on a particular graph  $G$  is sufficiently high, TrustGeoGen selects this data as the basis for the subsequent iteration's initial scenario. Specifically, the process can be represented as  $P'_{base} = P = \{p_{i+m}^g, p_{j+n}^d\}$ , where  $P$  serves as the starting point. The Constructor then incrementally adds new premises to this foundation, increasing the complexity of the scenario. This leads to the generation of  $P' = \{p_{i+m+x}^g, p_{j+n+y}^d\}$ . Following this, the Reasoner, Sampler, and Translator collaboratively work to complete graph construction, problem-solving, and translation, ultimately producing a new batch of high-quality data.

### 3.3 Multi-solution Data

In the field of GPS, exploring multiple solutions to a given problem is a crucial method for understanding geometric

**Algorithm 2: GeoExplore-M**


---

**Require:** Reasoning graph  $\mathcal{G} = (S, S_0, R, \hookrightarrow)$ , target statement  $s_n$ , threshold  $\tau_l$ , threshold  $\tau_r$ , number of searches  $n$

**Ensure:** Set of filtered reasoning paths  $\mathcal{P}_{\text{set}}$

- 1 **Initialize**  $\mathcal{P}_{\text{set}} \leftarrow \emptyset$ ;
- 2 **Initialize** used\_options  $\leftarrow \emptyset$ ;
- 3 **while** True **do**
- 4     **Initialize**  $\mathcal{P} \leftarrow \emptyset$ ;
- 5      $s \leftarrow s_n$ ;
- 6     **while**  $s \notin S_0$  **do**
- 7         Identify set of rules  $\mathcal{R}_s \subseteq R$  and corresponding parent statement sets  $S_{i-1}^m \subseteq S$  such that  $\forall r_s \in \mathcal{R}_s, \exists S_{i-1} \in S_{i-1}^m : S_{i-1} \xrightarrow{r_s} s$ ;
- 8         Select  $r_s \in \mathcal{R}_s$  and  $S_{i-1} \in S_{i-1}^m$  (choose different options in different searches);
- 9         used\_options  $\leftarrow$  used\_options  $\cup \{(r_s, S_{i-1})\}$ ;
- 10        **if**  $(S_{i-1}, r_s, s) \notin \mathcal{P}$  **then**
- 11           $\mathcal{P} \leftarrow \mathcal{P} \cup (S_{i-1}, r_s, s)$ ;
- 12         $s \leftarrow S_{i-1}$ ;
- 13     Assess path length:  $L \leftarrow |\mathcal{P}|$ ;
- 14     Compute premises ratio:  $R_P \leftarrow |S_P|/|S_0|$ , where  $S_P \subseteq \mathcal{P}$ ;
- 15     **if**  $L \geq \tau_l$  **and**  $R_P \geq \tau_r$  **then**
- 16          $\mathcal{P}_{\text{set}} \leftarrow \mathcal{P}_{\text{set}} \cup \{\mathcal{P}\}$ ;
- 17     **if** used\_options contains all possible options **then**
- 18         **Break**;
- 19 **return**  $\mathcal{P}_{\text{set}}$ ;

---

relationships in depth. By investigating different solution logics, a model can examine geometric scenarios from various perspectives, achieving a comprehensive understanding of the relationships among geometric elements. TrustGeoGen facilitates the construction of multi-solution datasets for specific geometric scenarios through the graph-building procedure of the modify Reasoner and the solving procedure of the Sampler.

During the graph construction phase, in order to obtain multiple solutions, for each statement  $s$ , when the Reasoner repeatedly identifies transitions in the form  $S_r \xrightarrow{r} s$ , each identified transition is retained. This retention of multiple transitions provides potential paths for exploring diverse solutions. In the solving process, the Sampler employs an adaptive search algorithm to generate reasoning paths. For any given problem  $s_n$ , the Sampler performs multiple path searches. If a statement  $s_i$  has multiple outgoing transitions, the Sampler selects a different transition at each iteration for the next reasoning step. Consequently, the reasoning paths obtained during these iterations will differ. It is worth noting that to ensure the generated reasoning paths are acyclic, the Sampler enforces a constraint during path construction. Specifically, when attempting to add a triplet  $(S_i, r_s, s)$  to the reasoning path  $\mathcal{P}$ , the Sampler checks whether this triplet already exists in  $\mathcal{P}$ . If it does, the statement  $s$  is not revisited, thereby preventing cyclical paths in the reasoning process. For details of the multi-solution path searching algorithm,

**Algorithm 3: GeoExplore-T**


---

**Require:** Directed graph  $\mathcal{G} = (S, S_0, R, \hookrightarrow)$ , target statement  $s_t \in S$ , threshold  $\tau_p$

**Ensure:** Trace-back reasoning data  $\mathcal{D}$

- 1 **Initialize**  $\mathcal{D} \leftarrow \emptyset$ ;
- 2 **Compute** all reasoning paths  $\mathcal{P}_{\text{set}}^t = \{\mathcal{P}_1^t, \mathcal{P}_2^t, \dots\}$  to  $s_t$  using algorithm 2;
- 3 **Randomly sample** a statement  $s_e \in S$  such that  $s_e \notin \text{UpstreamDependencies}(\mathcal{P}^t)$  for any  $\mathcal{P}^t \in \mathcal{P}_{\text{set}}^t$ ;
- 4 **Search** for a reasoning path  $\mathcal{P}^e$  leading to  $s_e$ ;
- 5 **if**  $\exists \mathcal{P}^t \in \mathcal{P}_{\text{set}}^t, \text{Overlap}(\mathcal{P}^e, \mathcal{P}^t) \geq \tau_p$  **then**
- 6      $\mathcal{D} \leftarrow \mathcal{D} \cup \mathcal{P}^e \cup \mathcal{P}^t$ ;
- 7 **return**  $\mathcal{D}$ ;

---

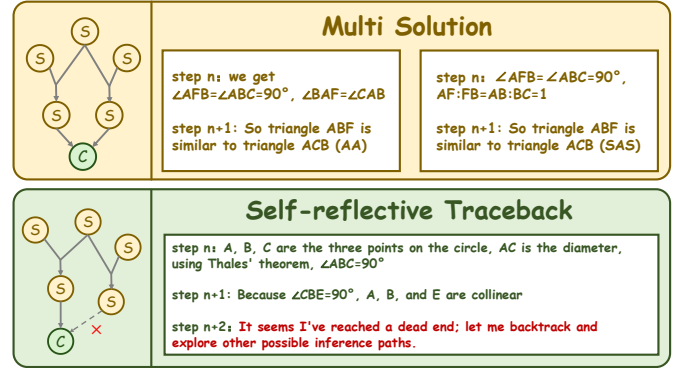


Fig. 3: Simple examples of Multi-solution and Self-reflective traceback data.

GeoExplore-M, refer to algorithm 2.

### 3.4 Self-reflective Traceback Data

Recent studies on the reasoning capabilities of large models suggest that these models acquire substantial knowledge during the pre-training phase. By providing training data with various cognitive templates during the post-training phase, the models can better utilize their inherent knowledge, thereby enhancing reasoning ability and improving response quality[47, 48]. Among these cognitive templates, self-reflection trace-back reasoning serve as highly effective approaches. However, self-reflection and retrospective reasoning often occur during the author's cognitive process and are rarely preserved in the final outputs, making the collection of relevant data particularly challenging. These types of data are even more scarce in the domain of multi-modal geometric problem-solving.

TrustGeoGen defines trace-back reasoning data as a sub-graph of  $\mathcal{G} = (S, S_0, R, \hookrightarrow)$ , characterized as the union of sub-graphs with identical upstream dependencies but differing final statement. Specifically, for a given piece of trace-back reasoning data, the process involves first deriving an incorrect final statement, then retrospectively navigating a correct reasoning path (shared by both the incorrect and correct paths), and ultimately arriving at the correct final statement. To achieve this, TrustGeoGen selects a target statement  $s_t$  and employs algorithm 2 to enumerate all possible reasoning paths  $\mathcal{P}^t \in \mathcal{P}_{\text{set}}^t$ . Next, a statement  $s_e$  is randomly sampled from the statement set  $S$ , ensuring that

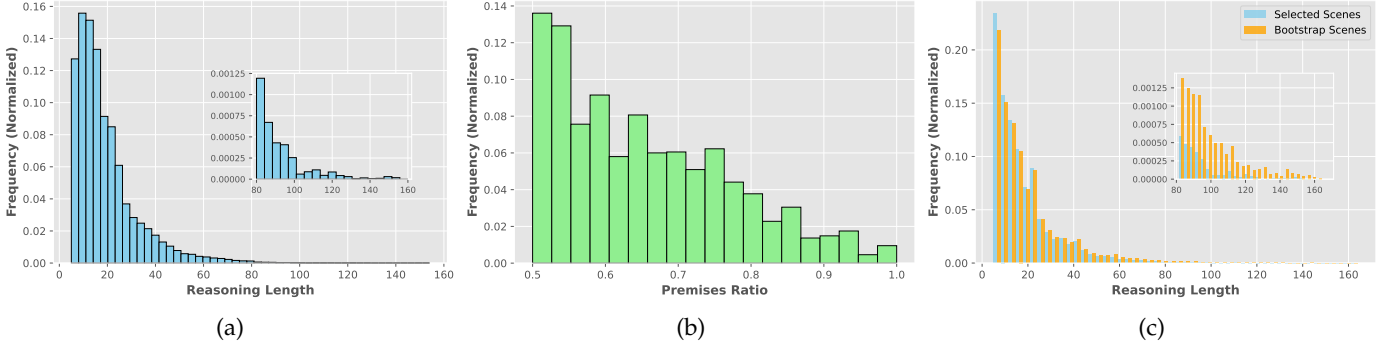


Fig. 4: Data distribution and augmentation. (a) Distribution of reasoning lengths, with most samples below 60 steps and a sharp decline beyond 80; the zoomed-in view highlights the ultra-long reasoning range. (b) Distribution of premise ratios, reflecting variability in logical dependencies. (c) Comparison of reasoning lengths before and after bootstrap augmentation, showing increased deep-reasoning samples (reasoning length  $\geq 40$ ) and reduced shallow ones.

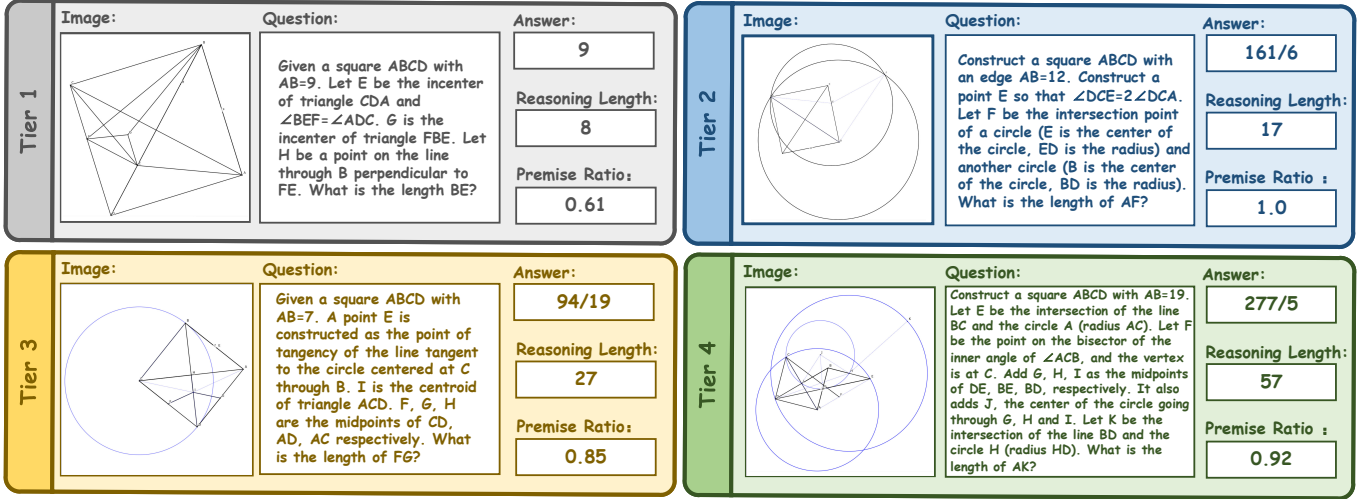


Fig. 5: Visualization examples of different difficulty levels in *GeoTrust-test*, where "reasoning length" indicates step length of reasoning path and "premise ratio" refer to the ratio of premises unutilized during formal reasoning and premises provided in the question.

$s_e$  does not belong to the upstream dependencies of any  $\mathcal{P}^t$ . Subsequently, TrustGeoGen searches for a reasoning path  $\mathcal{P}^e$  leading to  $s_e$ . If  $\mathcal{P}^e$  overlaps with any  $\mathcal{P}^t \in \mathcal{P}_{\text{set}}^t$  and the overlapping portions exceed the threshold  $\tau_p$ , TrustGeoGen outputs  $\mathcal{P}^e \cup \mathcal{P}^t$  as trace-back reasoning data. Notably, algorithm 2 is utilized to identify all possible reasoning paths for  $s_t$  to ensure that  $s_e$  does not appear in any potential upstream dependencies, maintaining the integrity of the reasoning process leading to  $s_t$ . The details of the trace-back data acquisition algorithm, *GeoExplore-T*, are presented in algorithm 3.

## 4 DATA ANALYSIS

The modality-completed trustworthy geometric reasoning data holds great potential for improving the geometric problem-solving capabilities of MLLMs. Moreover, it could generalize these abilities to other tasks requiring deep reasoning. To validate it, we utilized TrustGeoGen to produce the dataset *GeoTrust* of 200K raw samples<sup>3</sup>, from which 8K were sampled as the training set. Additionally, we employed different thresholds,  $\tau_l$  and  $\tau_r$ , in conjunction with manual

screening to curate a testset, *GeoTrust-test*, with 240 samples of varying levels of difficulty.

### 4.1 Data Distribution

TrustGeoGen was executed on a 60-core Intel Xeon (32) CPU @ 2.900GHz for two days, generating an initial dataset of 200K geometric reasoning instances in formal language. During the data generation process, we set the two filtering thresholds in the Sampler to  $\tau_l = 5$  and  $\tau_r = 0.5$ , respectively. The distributions of the reasoning length and premises ratio for the resulting 200K data are illustrated in fig. 4a and fig. 4b, respectively. The majority of the data is concentrated in the region where the reasoning length is less than 60, and it decreases sharply beyond 80. However, a small portion of the data exhibits reasoning lengths exceeding 150, indicating a considerably high level of reasoning complexity. For a more detailed view of the distribution, please refer to the zoomed-in section of fig. 4a.

### 4.2 Deep Reasoning Augmentation

As mentioned earlier, the randomly constructed scenarios by TrustGeoGen exhibit a rapid decline in reasoning length

3. Raw samples refers to the data which is not processed by translator

TABLE 2: Performance of state-of-the-art multi-modal language models on *GeoTrust-test*, which is divided into four difficulty levels. The best results are highlighted in **bold**, and the second best results are highlighted with an underline.

Model	#Params	Total (out of 240)		<i>Tier</i> <sub>1</sub> (out of 60)		<i>Tier</i> <sub>2</sub> (out of 60)		<i>Tier</i> <sub>3</sub> (out of 60)		<i>Tier</i> <sub>4</sub> (out of 60)	
		Count	Accuracy	Count	Accuracy	Count	Accuracy	Count	Accuracy	Count	Accuracy
LLaVA-1.5-7B [25]	7B	4	1.67%	3	5.00%	1	0.42%	0	0.00%	0	0.00%
Qwen2-VL-7B [42]	7B	11	4.58%	5	8.33%	2	3.33%	2	3.33%	2	3.33%
GPT-4o [30]	-	62	25.83%	31	51.67%	10	16.67%	11	18.33%	10	16.67%
Claude-3.7-sonnet [3]	-	66	27.50%	33	55.00%	16	26.67%	10	16.67%	7	11.67%
Qwen2.5-VL-72B [6]	72B	68	28.33%	32	53.33%	15	25.00%	15	25.00%	6	10.00%
DeepSeek-R1 * [13]	671B	89	37.08%	30	50.00%	20	33.33%	22	36.67%	17	28.33%
Intern-S1 [5]	235B+6B	<u>104</u>	<u>43.33%</u>	<u>35</u>	<u>58.33%</u>	<u>21</u>	<u>35.00%</u>	<u>25</u>	<u>41.67%</u>	<b>23</b>	<b>38.33%</b>
Gemini-2.5-pro [12]	-	<u>104</u>	43.33%	34	56.67%	<b>24</b>	<b>40.00%</b>	<b>26</b>	<b>43.33%</b>	<u>20</u>	33.33%
OpenAI-o3 [31]	-	<b>110</b>	<b>45.83%</b>	<b>37</b>	<b>61.67%</b>	<b>24</b>	<b>40.00%</b>	<b>26</b>	<b>43.33%</b>	<b>23</b>	<b>38.33%</b>

\* For DeepSeek-R1, we only provide natural language questions, but no images.

within the ultra-long range, posing challenges for generating deep-reasoning problems. To address this, we selected 226 samples with the longest reasoning lengths from an initial dataset of 200K and applied bootstrap augmentation to increase the proportion of deep-reasoning problems. Finally we obtained 376 geometric scenes after applying the bootstrap method. As shown in fig. 4c, after the bootstrap process, the data distribution in the region where reasoning length is smaller than 40 decreased, while it increased in the region where reasoning length is larger than 40. This method can be repeatedly applied to efficiently construct reasoning problems with significant depth and complexity.

### 4.3 Construction and Analysis of GeoTrust-Test

The synthetic data generated by TrustGeoGen can also be utilized to evaluate a model’s capabilities in the domain of deep geometric reasoning. From an initial dataset of 200K samples, we manually curated a set of 240 high-quality problems as the test set, graded by different levels of difficulty. Unlike the training data, which incorporates a mix of proof and solution-type problems, the *GeoTrust-test* is composed exclusively of problems with numerical solutions to simplify the evaluation process. As shown in fig. 5, these problems are divided into four tiers, with each tier containing 60 problems. The reasoning lengths for *Tier*<sub>1</sub> range from 5 to 10 steps, *Tier*<sub>2</sub> spans from 10 to 20 steps, *Tier*<sub>3</sub> ranges from 20 to 50 steps, and *Tier*<sub>4</sub> exceeds 50 steps. It is worth noting that, to introduce distractors into the questions, the premises provided may not necessarily all be utilized in the reasoning process, resulting in a potentially lower premise ratio.

## 5 EXPERIMENTS

To validate the quality and effectiveness of the geometric Problem Solving data generated by TrustGeoGen, we conducted experiments to explore:

- Whether existing MLLMs demonstrate competent performance on complex geometric problems?
- Whether the data generated by TrustGeoGen have sufficient complexity to provide gains for SOTA models?
- Whether geometric reasoning data with rigorous formal verification improve MLLMs’ capabilities and provide specific advantages?

- Whether *GeoTrust*, constructed without prior data sources, can generalize to OOD geometric testset?

### 5.1 Dataset, Metric, and Implementation Detail

**Dataset.** To evaluate the capability of MLLMs in solving complex geometry problems, we construct *GeoTrust-test* by partitioning the original *GeoTrust* dataset. As introduced in section 4.3, the testset *GeoTrust-test* comprehensively covers four difficulty levels ranging from *Tier*<sub>1</sub> to *Tier*<sub>4</sub>. To validate the effectiveness of our data construction, we additionally sample 2342 geometry problems as *GeoTrust-train*, with different difficulty tier.

**Metric.** To eliminate potential evaluation bias introduced by the multiple-choice format, all input questions in the experiments are presented without answer options. Both the model’s final output answers and GT labels are extracted and converted into floating-point values for numerical comparison, with a relative error tolerance of 1% permitted.

**Implementation Detail.** In the experimental training protocol, all models are trained through supervised fine-tuning (SFT) with full-parameter updates for one epoch to prevent overfitting. All training and evaluation processes are conducted on 8 NVIDIA A100 (80G) GPUs.

### 5.2 Performance of Existing MLLMs

As shown in table 2, the experimental results from the *GeoTrust-test* testset reveal critical insights into the capabilities of MLLMs in tackling complex geometric problems. Existing open-source models, such as Qwen2-VL-7B, demonstrate significant limitations, achieving only a 4.58% overall accuracy (11/240), which also underscores the inherent challenges of the dataset and confirms its independence from prior biases in existing open-source testsets. The closed-source reasoning model, OpenAI-o3, demonstrated the strongest geometric reasoning capability, solving 110 problems with an accuracy of 45.83%. Furthermore, models that have undergone "deep thinking" training (e.g., OpenAI-o3, Gemini-2.5-pro, Intern-S1, DeepSeek-R1) exhibited a more gradual decline in accuracy as problem difficulty increased (from *Tier*<sub>1</sub> to *Tier*<sub>4</sub>). In contrast, models without such specialized training (e.g., GPT-4o, Claude-3.7-sonnet, Qwen2.5-VL-72B) experienced a sharp drop in accuracy on more challenging problems. This distinction underscores the critical importance of deep reasoning abilities for GPS. The



TABLE 3: Complexity comparison between different benchmarks. The most difficult results are highlighted in **bold**, and the second difficult results are highlighted with an underline. It is indicated that our geometry constructed problems are more challenging for most mainstream MLLMs.

Model	Release Date	GeoQA (mid-school level)	Geometry3K (mid-school level)	OlympiadBench-Geo (olympiad level)	GeoTrust-test
GPT-4o [30]	May, 2024	42.31%	31.45%	<b>13.39%</b>	<u>25.83%</u>
Claude-3.7-sonnet [3]	Feb, 2025	49.73%	33.28%	<b>17.86%</b>	<u>27.50%</u>
Qwen2.5-VL-72B [6]	Jan, 2025	67.90%	35.44%	<u>29.46%</u>	<b>28.33%</b>
Intern-S1 [5]	Jul, 2025	62.47%	52.31%	<u>49.11%</u>	<b>43.33%</b>
Gemini-2.5-pro[12]	Jun, 2025	79.58%	80.70%	<u>75.00%</u>	<b>43.33%</b>
OpenAI-o3 [31]	Apr, 2025	79.31%	81.03%	<u>77.68%</u>	<b>45.83%</b>

consistent decrease in accuracy across all models with rising difficulty collectively emphasizes the need for enhanced reasoning architectures and training paradigms to address the steep complexity gradient in geometric problem solving.

### 5.3 Complexity Analysis Between Benchmarks

Although constructing geometric data using formal engines can enhance acquisition efficiency, it presents challenges in ascertaining the data’s complexity and its actual contribution to model training. To address this, TrustGeoGen utilizes filtering parameters,  $\tau_l$  and  $\tau_r$ , to screen for problems of varying difficulty, thereby enabling the selective generation of data that provides tangible benefits to the model. As detailed in table 3, we evaluated several state-of-the-art (SOTA) multimodal large language models on four distinct geometry benchmarks to assess their respective complexity. The performance of SOTA models indicates that *GeoTrust-test* presents a level of difficulty comparable to OlympiadBench-Geo, with models generally struggling to achieve high scores on either. Notably, even well-pretrained models like Gemini-2.5-pro and OpenAI-o3, which exhibit substantially improved accuracy on OlympiadBench-Geo thanks to extensive pre-training on geometry data, still fail to surpass the 50% accuracy mark on *GeoTrust-test*. This underscores the potential of **TrustGeoGen** to further boost the performance of these advanced models by providing a continuous stream of fresh and challenging data.

### 5.4 Effectiveness Analysis of Trustworthy Data

TrustGeoGen constructs trustworthy geometric reasoning data using a formal engine. It bridges the gap between formal and human-like reasoning through "connection thinking" (line 12). Furthermore, thinking template data—comprising multi-solution data (section 3.3) and self-reflective traceback data (section 3.4)—is utilized to introduce diverse reasoning pathways. In this section, we design comprehensive experiments to validate the effectiveness of our trustworthy data.

#### 5.4.1 Necessary of Connection Thinking

We conducted experiments to validate our data’s effectiveness using four models: LLaVA-1.5-7B, LLaVA-1.5-13B, Qwen2-VL-2B, and Qwen2-VL-7B. Each model was fine-tuned via Supervised Fine-Tuning (SFT) on a sampled dataset of 2,158 instances. We applied two distinct training strategies separately: one using the NL translation data

and the other using the connection thinking data, both of which are detailed in fig. 2. All fine-tuned models were subsequently evaluated on the *GeoTrust-test* benchmark.

As shown in table 4, the results demonstrate that both training approaches lead to a significant increase in model accuracy. Notably, the models trained with the connection thinking data exhibited a more substantial improvement, consistently achieving accuracy gains of over 10%.

Furthermore, we analyzed the outputs of models trained on different datasets. As illustrated in fig. 6, there is a substantial difference in the content generated by models trained on the two respective datasets. The model trained on the "NL Translation" data tends to produce repetitive content and exhibits apparent logical fallacies. In contrast, the model trained on our proposed "connection thinking" data generates outputs that are significantly more coherent and logically sound.

The "NL Translation" data suffers from two key limitations that prevent a model from truly acquiring reasoning capabilities. First, its formal-language reasoning steps are highly structured, merely presenting premises, applied theorems, and derived conclusions in a templated format without elucidating the underlying rationale of the proof process. A model trained on such data learns to replicate theorems it has seen rather than how to apply them proficiently. Second, a significant gap exists between this formal reasoning process and authentic human-like reasoning, as there are no explicit logical connections between adjacent steps. Consequently, each subsequent step appears to emerge abruptly, lacking logical coherence.

To address these limitations, our "connection thinking" approach uses the "NL Translation" data as a foundational skeleton but augments it by inserting a detailed thought process between each pair of consecutive reasoning steps. This enrichment not only explains each step in detail but also articulates the logical link between them by considering previously established conclusions and the ultimate goal. This enriched data structure enables the model to master the application of plane geometry theorems, thereby significantly improving its geometric problem-solving capabilities.

#### 5.4.2 Advantages Provided by Trustworthy Data

To validate the effectiveness of data generated by TrustGeoGen, we conducted a comparative experiment using pseudo-labeled data. We fed 2,158 questions generated by TrustGeoGen into OpenAI-o3 [31] and obtained answers from the model. The responses were then evaluated using

TABLE 4: Translation performance comparison across different models and training data sources. The  $\Delta$  column indicates the improvement over the "Pretraining" baseline. Improvements are marked with an upward arrow ( $\uparrow$ ).

Training Data	LLaVA-1.5-7B		LLaVA-1.5-13B		Qwen2-VL-2B		Qwen2-VL-7B	
	Accuracy	$\Delta$	Accuracy	$\Delta$	Accuracy	$\Delta$	Accuracy	$\Delta$
Pretraining	1.67% (4)	-	2.08% (5)	-	3.33% (8)	-	4.58% (11)	-
NL Translation	6.25% (15)	4.58% $\uparrow$	6.67% (16)	4.59% $\uparrow$	8.75% (21)	5.42% $\uparrow$	8.75% (21)	4.17% $\uparrow$
Connection Thinking	15.42% (37)	13.75% $\uparrow$	19.17% (46)	17.09% $\uparrow$	13.75% (33)	10.42% $\uparrow$	21.67% (52)	17.09% $\uparrow$

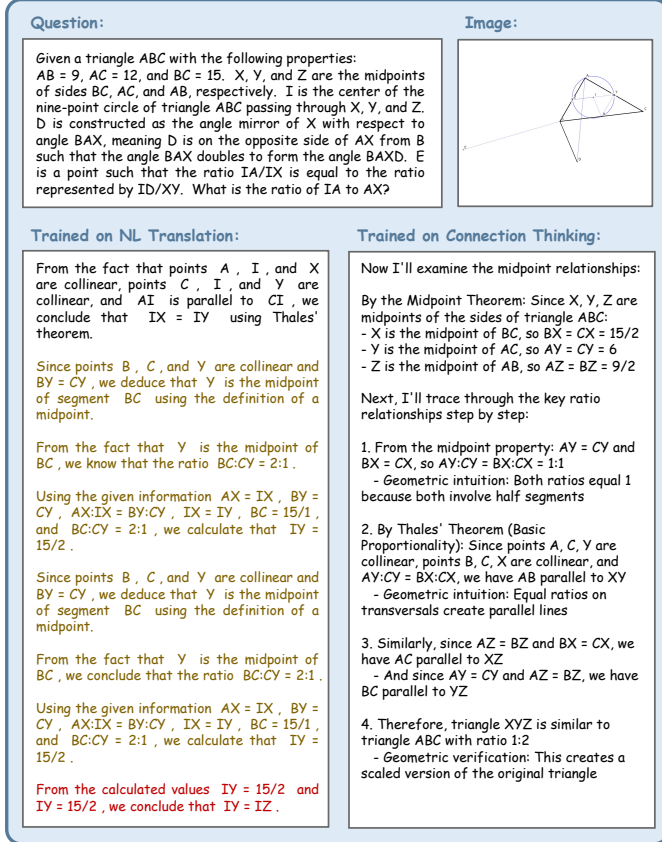


Fig. 6: Fragments of model's response: The response of model trained on NL Translation dataset is **repeating & illogical**, while the response of model trained on Connection Thinking dataset is reasonable and clear.

the metrics described in section 5.1, resulting in 846 correctly answered questions, which we treat as pseudo-labeled data. For fairness, we also used the same 846 questions as the GeoTrust Data in our experiments.

We trained four models using the pseudo-labeled data and GeoTrust data with varying proportions (100%, 50%, 30%, and 10%). The trained models were subsequently tested on the GeoTrust-test set. As shown in table 5, the model trained with 100% GeoTrust data slightly outperformed the model trained with pseudo-labeled data. This indicates that, given the same data volume, the synthetic data generated by TrustGeoGen achieves comparable or even superior results compared to pseudo-labeled data produced by SOTA models. It is worth noting that the SOTA model did not correctly answer all TrustGeoGen-generated questions, whereas TrustGeoGen can generate large volumes of data accompanied by accurate solution processes, providing a significant advantage for model training. Furthermore, the

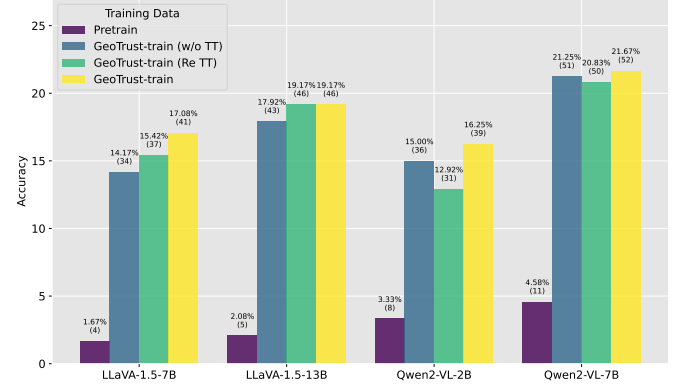


Fig. 7: Ablation Study of Thinking Template on GeoTrust-test

experimental results demonstrate that the model's performance consistently improves with increasing training data size, further confirming the effectiveness of our generated data.

#### 5.4.3 Advantages of by Thinking Template

We investigated the impact of our proposed thinking template across four model architectures. Our primary training dataset, GeoTrust-train, was constructed by augmenting a baseline dataset of 2,158 instances with 184 instances that incorporate the thinking template, resulting in a total of 2,342 instances. To isolate the contribution of the Thinking Template, we created three training setups:

- *GeoTrust-train (w/o TT)*: This version consists solely of the 2,158 baseline instances, with all Thinking Template data removed.
- *GeoTrust-train (Re TT)*: To maintain the dataset size for a fair comparison, this version replaces the 184 Thinking Template instances with 184 additional baseline instances, also totaling 2,342 instances.
- *GeoTrust-train*: This is the full dataset including both the 2,158 baseline instances and the 184 Thinking Template instances.

Subsequently, each of the three resulting models was evaluated on the GeoTrust-test to assess their performance.

Fig. 7 illustrates the experimental results on the Thinking Template dataset. The Thinking Template demonstrates enhanced performance across all four models. Interestingly, for the LLaVA-1.5 series, the model trained with our Thinking Template (Re TT) consistently outperformed the version trained without it (w/o TT). In contrast, for the Qwen2-VL series, the model trained without the Thinking Template (w/o TT) achieved superior results.

TABLE 5: Performance comparison using different data augmentation strategies. "Pseudo-labels" and various percentages of "Our data" are compared against the "Pretraining" baseline. The  $\Delta$  column shows the improvement over the baseline. Improvements are marked with an upward arrow ( $\uparrow$ ).

Training data	LLaVA-1.5-7B		LLaVA-1.5-13B		Qwen2-VL-2B		Qwen2-VL-7B	
	Accuracy	$\Delta$	Accuracy	$\Delta$	Accuracy	$\Delta$	Accuracy	$\Delta$
Pretraining	1.67%(4)	-	2.08%(5)	-	3.33%(8)	-	4.58%(11)	-
Pseudo-labels data	12.08%(29)	10.42% $\uparrow$	13.75%(33)	11.67% $\uparrow$	11.25%(27)	7.92% $\uparrow$	12.92%(31)	8.33% $\uparrow$
GeoTrust data 10%	5.83%(14)	4.17% $\uparrow$	7.50%(18)	5.42% $\uparrow$	3.75%(9)	0.42% $\uparrow$	11.25%(27)	6.67% $\uparrow$
GeoTrust data 30%	9.17%(22)	7.50% $\uparrow$	10.83%(26)	8.75% $\uparrow$	10.42%(25)	7.08% $\uparrow$	12.08%(29)	7.50% $\uparrow$
GeoTrust data 50%	9.58%(23)	7.92% $\uparrow$	11.25%(27)	9.17% $\uparrow$	10.00%(24)	6.67% $\uparrow$	12.50%(30)	7.92% $\uparrow$
GeoTrust data 100%	12.92%(31)	11.25% $\uparrow$	14.17%(34)	12.08% $\uparrow$	12.50%(30)	9.17% $\uparrow$	14.17%(34)	9.58% $\uparrow$

## 5.5 OOD Generalization

We evaluated the efficacy of TrustGeoGen in enhancing GPS performance by conducting extensive experiments across three diverse out-of-domain (OOD) benchmarks: GeoQA, Geometry3k, and OlympiadBench. These datasets were strategically chosen to cover a wide spectrum of challenges. GeoQA, sourced from real-world scenarios, offers diverse and unstructured problems accompanied by rich natural language rationales. Geometry3k provides formally structured problems generated via a formal engine, but without natural language explanations. To assess performance on highly complex tasks, we included OlympiadBench, which contains challenging competition-level problems. Together, this suite of benchmarks enables a robust and comprehensive evaluation of our approach.

### 5.5.1 GeoQA

The GeoQA dataset originates from real-world sources and comprises a high-quality, diverse set of problems presented in natural language along with their corresponding solutions. The dataset provides a training partition of 3,499 problems and a test partition of 754. In our experiments, we fine-tuned four distinct models via Supervised Fine-Tuning (SFT) utilizing three separate training datasets: the GeoQA training data, the *GeoTrust-train* data, and a combined dataset. Subsequently, we assessed the models' efficacy on the GeoQA test set.

The results, presented in table 6, indicate that for the LLaVA-1.5 model family, all three training approaches yielded performance enhancements. It is particularly noteworthy that *GeoTrust-train*, despite being from a different domain, still enabled the models to achieve superior results on GeoQA. Moreover, a synergistic effect was observed when the two datasets were merged, with *GeoTrust-train* offering further incremental gains.

In contrast, for the Qwen2-VL model family, fine-tuning exclusively on the *GeoTrust-train* data led to performance degradation. A plausible explanation is that the Qwen2-VL series, being more recent, already possesses strong geometric reasoning abilities from extensive pre-training. This strong prior knowledge explains its superior initial performance, but also makes it susceptible to performance loss when adapted to a dataset with a distinct data distribution like *GeoTrust-train*. Despite this, using *GeoTrust-train* as a supplementary dataset for GeoQA still enhanced the models' performance.

TABLE 6: Performance comparison on GeoQA dataset using different training data mixture. The  $\Delta$  column indicates the improvement over the baseline. An up-arrow ( $\uparrow$ ) indicates an improvement, and a down-arrow ( $\downarrow$ ) indicates a decline.

Model	Training Data	Accuracy	$\Delta$
LLaVA-1.5-7B	-	13.66% (103)	-
	GeoQA	24.80% (187)	+11.14% $\uparrow$
	GeoTrust-train	13.79% (104)	+0.13% $\uparrow$
	GeoQA+GeoTrust-train	26.92% (203)	+13.26% $\uparrow$
LLaVA-1.5-13B	-	16.31% (123)	-
	GeoQA	25.46% (192)	+9.15% $\uparrow$
	GeoTrust-train	16.71% (126)	+4.00% $\uparrow$
	GeoQA+GeoTrust-train	30.11% (227)	+13.80% $\uparrow$
Qwen2-VL-2B	-	20.56% (155)	-
	GeoQA	25.46% (192)	+4.90% $\uparrow$
	GeoTrust-train	14.99% (113)	-5.57% $\downarrow$
	GeoQA+GeoTrust-train	27.72% (209)	+7.16% $\uparrow$
Qwen2-VL-7B	-	37.00% (279)	-
	GeoQA	39.66% (299)	+2.66% $\uparrow$
	GeoTrust-train	28.38% (214)	-8.62% $\downarrow$
	GeoQA+GeoTrust-train	43.50% (328)	+6.50% $\uparrow$

GeoQA was evaluated in a direct question-answering (QA) format, rather than a multiple-choice setting. The same metrics as described in section 5.1 were used.

### 5.5.2 Geometry3K

Geometry3K, a dataset constructed via a formal engine for solving geometry problems with formal language, comprises 2,101 training and 601 test examples. We performed SFT experiments on this data using different mixtures, and the results are summarized in table 7. For the LLaVA-1.5-7B, LLaVA-1.5-13B, and Qwen2-VL-2B models, every data mixture enhanced performance. Conversely, on Qwen2-VL-7B, training solely on Geometry3K led to a decline in performance. This performance drop persisted even when the training data was supplemented with *GeoTrust-train*.

Qwen2-VL-7B's strong pre-trained performance on Geometry3K is characteristic of a well-saturated large multimodal model. This suggests that for such models, fine-tuning on data with a similar distribution to the pre-training set can paradoxically lead to performance degradation. Conversely, the smaller Qwen2-VL-2B model, whose pre-training was likely less saturated, still demonstrated further gains when fine-tuned on this data.

### 5.5.3 OlympiadBench-geo

OlympiadBench serves as an Olympiad-level benchmark comprising authentic competition problems to assess the multimodal reasoning capabilities of foundation models.

TABLE 7: Performance comparison on Geometry3k using different training data mixture.

Model	Training Data	Accuracy	$\Delta$
LLaVA-1.5-7B	-	1.16% (7)	-
	Geometry3K	6.66% (40)	+5.50% $\uparrow$
	GeoTrust-train	2.83% (17)	+1.67% $\uparrow$
	Geometry3K+GeoTrust-train	7.99% (48)	+6.83% $\uparrow$
LLaVA-1.5-13B	-	2.33% (14)	-
	Geometry3K	7.32% (44)	+4.99% $\uparrow$
	GeoTrust-train	3.33% (20)	+1.00% $\uparrow$
	Geometry3K+GeoTrust-train	8.65% (52)	+6.32% $\uparrow$
Qwen2-VL-2B	-	8.32% (50)	-
	Geometry3K	10.15% (61)	+1.83% $\uparrow$
	GeoTrust-train	8.65% (52)	+0.33% $\uparrow$
	Geometry3K+GeoTrust-train	12.15% (73)	+3.83% $\uparrow$
Qwen2-VL-7B	-	17.97% (108)	-
	Geometry3K	15.80% (95)	-2.17% $\downarrow$
	GeoTrust-train	19.13% (115)	+1.16% $\uparrow$
	Geometry3K+GeoTrust-train	16.14% (97)	-1.83% $\downarrow$

Geometry3K was evaluated in a direct QA format, rather than a multiple-choice setting. The same metrics as described in section 5.1 were used.

TABLE 8: Performance comparison on OlympiadBench-geo using different training data mixture.

Model	Training Data	Accuracy	$\Delta$
LLaVA-1.5-7B	-	0.00% (0)	-
	GeoQA	3.57% (4)	+3.57% $\uparrow$
	GeoTrust-train	1.79% (2)	+1.79% $\uparrow$
	GeoQA+GeoTrust-train	3.57% (4)	+3.57% $\uparrow$
LLaVA-1.5-13B	-	1.79% (2)	-
	GeoQA	6.25% (7)	+4.46% $\uparrow$
	GeoTrust-train	2.68% (3)	+0.89% $\uparrow$
	GeoQA+GeoTrust-train	6.25% (7)	+4.46% $\uparrow$
Qwen2-VL-2B	-	2.68% (3)	-
	GeoQA	4.46% (5)	+1.78% $\uparrow$
	GeoTrust-train	4.46% (5)	+1.78% $\uparrow$
	GeoQA+GeoTrust-train	6.25% (7)	+3.57% $\uparrow$
Qwen2-VL-7B	-	7.14% (8)	-
	GeoQA	5.36% (6)	-1.78% $\downarrow$
	GeoTrust-train	9.82% (11)	+2.68% $\uparrow$
	GeoQA+GeoTrust-train	8.93% (10)	+1.79% $\uparrow$

For our evaluation, we designated a subset of 112 geometry problems from OlympiadBench as the test set OlympiadBench-geo to verify the efficacy of our proposed data. In the absence of a provided training set from OlympiadBench, we formulated several data compositions for our experiments by utilizing the training data from GeoQA.

The experimental results, presented in table 8, reveal a clear trend. Fine-tuning the four models exclusively on *GeoTrust-train* resulted in universal performance enhancements. However, for the Qwen2-VL-7B model, reliance on GeoQA data alone caused a decline in performance—a phenomenon likely associated with data distribution issues with its pre-training data, as discussed in previous sections. Crucially, combining the GeoQA and *GeoTrust-train* datasets produced marked performance improvements across all models, demonstrating their enhanced problem-solving abilities on this demanding benchmark.

#### 5.5.4 Ablation Study of Thinking Template

As established in the preceding sections, our *GeoTrust-train* dataset is composed of two primary components: base data

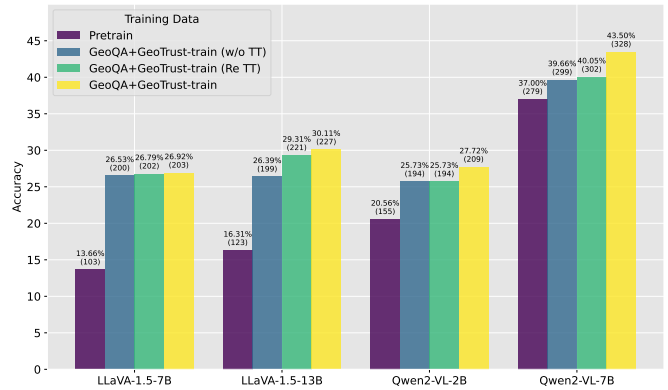


Fig. 8: Ablation Study of Thinking Template on GeoQA

and thinking template (TT) data. To validate the effectiveness of the thinking template data, we conduct a series of ablation studies on the GeoQA and Geometry3K datasets. Following the same methodology outlined in section 5.4.3, we partition the *GeoTrust-train* data into three distinct configurations for our experiments: without thinking templates (w/o TT), replace thinking templates (Re TT), and full data. Each configuration is then combined with the training sets of GeoQA and Geometry3K, respectively, to fine-tune the models. The models are subsequently evaluated on the corresponding test sets.

The experimental results on GeoQA, illustrated in fig. 8, reveal that the inclusion of thinking templates consistently enhances performance across all models. For LLaVA-1.5-7B, however, the addition of more data, including thinking templates, yields only marginal improvements. This suggests that the model’s performance may have reached a saturation point with the base data alone. In contrast, LLaVA-1.5-13B demonstrates greater sensitivity to data volume; the performance gain from increasing the dataset size is more pronounced than that from introducing thinking templates. Conversely, the Qwen2-VL series benefits more significantly from the addition of thinking templates. This finding aligns with our earlier analysis that since these models are already well-pretrained, they are more responsive to novel data types than to a mere increase in data quantity.

The results on Geometry3K, as depicted in fig. 9, present a different pattern. Notably, Qwen2-VL-7B achieves the highest score out-of-the-box (i.e., with its original pre-training), a result we attribute to its pre-training data composition. Nevertheless, when fine-tuned on our mixed datasets, the inclusion of thinking templates still provides a clear performance boost. Overall, the thinking templates demonstrate a more pronounced impact on the performance of the LLaVA-1.5 series models in these experiments.

#### 5.5.5 Summary of Experiments Results

Our experiments OOD datasets and benchmarks confirm the generalizability of TrustGeoGen, demonstrating its ability to deliver consistent performance enhancements for models across diverse geometric datasets. A key component, "connection thinking", guarantees the logical coherence and variety of the synthesized data, to the extent that models trained solely on our *GeoTrust-train* dataset achieve



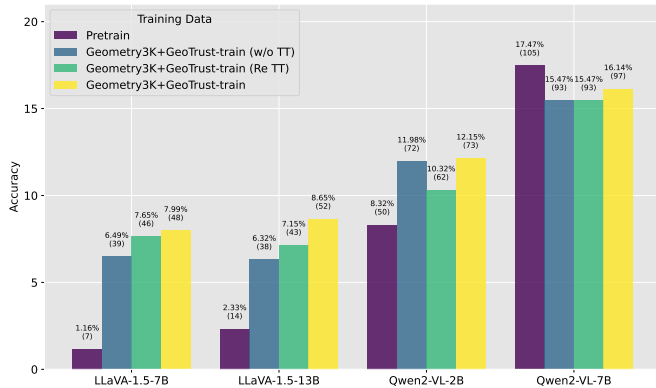


Fig. 9: Ablation Study of Thinking Template on Geometry3K

notable improvements. The evaluated models display intriguing and divergent behaviors. For instance, the LLaVA-1.5 family—representing an earlier generation of models trained with limited geometric data and less sophisticated methods—shows considerable potential for growth. Our synthetic data consistently and significantly elevates its accuracy. Conversely, the Qwen2-VL series, which leverages state-of-the-art training paradigms and extensive geometric data, is already well-pretrained for these tasks. Nevertheless, enriching its training regimen with *GeoTrust-train* still yields further performance gains.

Furthermore, our novel "thinking templates" introduce structured, multi-faceted problem-solving paradigms previously unseen by these models during pre-training. This explains why even the robustly pre-trained Qwen2-VL models derive clear and objective benefits from the templates' novel reasoning structures.

In summary, TrustGeoGen-synthesized data has demonstrated robust efficacy across a range of datasets and model architectures. Both of its core mechanisms, "connection thinking" and "thinking templates", have been proven effective. These results offer valuable insights and a compelling direction for future research on leveraging formal engines for automated data curation in training advanced models.

## 6 CONCLUSION AND FURTHER DISCUSSION

**Conclusion.** We have introduced TrustGeoGen, a multi-modal, integrated, and formal-verified engine for automatically generating fully geometric reasoning data. The resultant *GeoTrust* dataset demonstrates proven effectiveness and generalization capabilities. Furthermore, our benchmark, *GeoTrust-test*, reveals critical limitations in existing multimodal large language models (MLLMs) when handling complex geometric reasoning tasks. Notably, the proposed "connection thinking" bridges the gap between formal and natural reasoning, offering a valuable blueprint for synthesizing model training data with formal engines. In parallel, the "thinking template" mechanism enriches the diversity of the synthetic data, providing greater information gain and further enhancing the models' reasoning abilities. TrustGeoGen represents a crucial first step toward trustworthy geometric problem-solving, establishing a new paradigm for generating rigorous and reliable data.

**Further Discussion.** We hope that future research will develop from the following two perspectives:

**Trustworthy Geometric Problem Solving:** Models should produce verifiable reasoning steps, not merely correct answers. Achieving this demands both reliable data and robust evaluation mechanisms are required. Leveraging the generated data from TrustGeoGen, further study can focus on autoformalization approaches that translate natural language reasoning into formalized steps, enabling automated verification of each deduction's logical validity. Moreover, TrustGeoGen can dynamically generate evaluation data to prevent prior data leakage during evaluation, ensuring higher reliability in unseen geometric scenarios.

**Formal Enhanced Reasoning:** TrustGeoGen's formalized reasoning environment enables the generation of trustworthy geometric data by constructing rigorous reasoning graphs that ensure logical correctness at each step. These graphs provide a structured foundation for exploring diverse mathematical reasoning strategies through tailored sampling methods: the current work implements multi-solution and self-reflection traceback data, while future extensions could incorporate the idea of reverse thinking and categorical discussion, etc. These ideas could be further enhanced by integrating alternative training approaches (e.g. RL) to generalize to other reasoning scenarios.

## ACKNOWLEDGEMENTS

The research was supported by Shanghai Artificial Intelligence Laboratory, a locally commissioned task from the Shanghai Municipal Government, National Natural Science Foundation of China (Grant No. 92370201 and 62222607), and the Shanghai Municipal Science and Technology Major Project (Grant No. 22DZ1100102).

## REFERENCES

- [1] Josh Achiam, Steven Adler, Sandhini Agarwal, Lama Ahmad, Ilge Akkaya, Florencia Leoni Aleman, Diogo Almeida, Janko Altschmidt, Sam Altman, Shyamal Anadkat, et al. Gpt-4 technical report. *arXiv preprint arXiv:2303.08774*, 2023. 1
- [2] Josh Achiam, Steven Adler, Sandhini Agarwal, Lama Ahmad, Ilge Akkaya, Florencia Leoni Aleman, Diogo Almeida, Janko Altschmidt, Sam Altman, Shyamal Anadkat, et al. Gpt-4 technical report. *arXiv preprint arXiv:2303.08774*, 2023. 3
- [3] Anthropic. The claude 3 model family: Opus, sonnet, haiku. <https://www.anthropic.com/>, 2024. 8, 9
- [4] Jinze Bai, Shuai Bai, Shusheng Yang, Shijie Wang, Sinan Tan, Peng Wang, Junyang Lin, Chang Zhou, and Jingren Zhou. Qwen-vl: A frontier large vision-language model with versatile abilities. *arXiv preprint arXiv:2308.12966*, 2023. 1, 3
- [5] Lei Bai, Zhongrui Cai, Maosong Cao, Weihao Cao, Chiyu Chen, Haojiong Chen, Kai Chen, Pengcheng Chen, Ying Chen, Yongkang Chen, et al. Intern-s1: A scientific multimodal foundation model. *arXiv preprint arXiv:2508.15763*, 2025. 8, 9
- [6] Shuai Bai, Keqin Chen, Xuejing Liu, Jialin Wang, Wenbin Ge, Sibao Song, Kai Dang, Peng Wang, Shijie Wang,

- Jun Tang, Humen Zhong, Yuanzhi Zhu, Mingkun Yang, Zhaohai Li, Jianqiang Wan, Pengfei Wang, Wei Ding, Zheren Fu, Yiheng Xu, Jiabo Ye, Xi Zhang, Tianbao Xie, Zesen Cheng, Hang Zhang, Zhibo Yang, Haiyang Xu, and Junyang Lin. Qwen2.5-vl technical report. *ArXiv*, abs/2502.13923, 2024. 8, 9
- [7] Jie Cao and Jing Xiao. An augmented benchmark dataset for geometric question answering through dual parallel text encoding. In *Proceedings of the 29th International Conference on Computational Linguistics*, pages 1511–1520, 2022. 2, 3
- [8] Jiaqi Chen, Tong Li, Jinghui Qin, Pan Lu, Liang Lin, Chongyu Chen, and Xiaodan Liang. Unigeo: Unifying geometry logical reasoning via reformulating mathematical expression. In *Proceedings of the 2022 Conference on Empirical Methods in Natural Language Processing*, pages 3313–3323, 2022. 1, 2, 3
- [9] Jiaqi Chen, Jianheng Tang, Jinghui Qin, Xiaodan Liang, Lingbo Liu, Eric Xing, and Liang Lin. Geoqa: A geometric question answering benchmark towards multimodal numerical reasoning. In *Findings of the Association for Computational Linguistics: ACL-IJCNLP 2021*, pages 513–523, 2021. 1, 2, 3
- [10] Zhe Chen, Weiyun Wang, Hao Tian, Shenglong Ye, Zhangwei Gao, Erfei Cui, Wenwen Tong, Kongzhi Hu, Jiapeng Luo, Zheng Ma, et al. How far are we to gpt-4v? closing the gap to commercial multimodal models with open-source suites. *Science China Information Sciences*, 67(12):220101, 2024. 1
- [11] Yuri Chervonyi, Trieu H. Trinh, Miroslav Olšák, Xiaomeng Yang, Hoang Nguyen, Marcelo Menegali, Junehyuk Jung, Vikas Verma, Quoc V. Le, and Thang Luong. Gold-medalist performance in solving olympiad geometry with alphageometry2. *ArXiv*, 2502.03544, 2025. 1, 3
- [12] Gheorghe Comanici, Eric Bieber, Mike Schaekermann, Ice Pasupat, Noveen Sachdeva, Inderjit Dhillon, Marcel Blistein, Ori Ram, Dan Zhang, Evan Rosen, et al. Gemini 2.5: Pushing the frontier with advanced reasoning, multimodality, long context, and next generation agentic capabilities. *arXiv preprint arXiv:2507.06261*, 2025. 8, 9
- [13] DeepSeek-AI, Daya Guo, Dejian Yang, Haowei Zhang, Jun-Mei Song, Ruoyu Zhang, Runxin Xu, Qihao Zhu, Shirong Ma, Peiyi Wang, Xiaoling Bi, Xiaokang Zhang, Xingkai Yu, and et al. Deepseek-r1: Incentivizing reasoning capability in llms via reinforcement learning. *ArXiv*, abs/2501.12948, 2025. 8
- [14] Xiaoyi Dong, Pan Zhang, Yuhang Zang, Yuhang Cao, Bin Wang, Linke Ouyang, Xilin Wei, Songyang Zhang, Haodong Duan, Maosong Cao, Wenwei Zhang, Yining Li, Hang Yan, Yang Gao, Xinyue Zhang, Wei Li, Jingwen Li, Kai Chen, Conghui He, Xingcheng Zhang, Yu Qiao, Dahua Lin, and Jiaqi Wang. Internlm-xcomposer2: Mastering free-form text-image composition and comprehension in vision-language large model. *ArXiv*, abs/2401.16420, 2024. 1
- [15] Xiaoyi Dong, Pan Zhang, Yuhang Zang, Yuhang Cao, Bin Wang, Linke Ouyang, Songyang Zhang, Haodong Duan, Wenwei Zhang, Yining Li, Hang Yan, Yang Gao, Zhe Chen, Xinyue Zhang, Wei Li, Jingwen Li, Wenhai Wang, Kai Chen, Conghui He, Xingcheng Zhang, Jifeng Dai, Yu Qiao, Dahua Lin, and Jiaqi Wang. Internlm-xcomposer2-4khd: A pioneering large vision-language model handling resolutions from 336 pixels to 4k hd. *ArXiv*, abs/2404.06512, 2024. 1
- [16] Chaoyou Fu, Peixian Chen, Yunhang Shen, Yulei Qin, Mengdan Zhang, Xu Lin, Jinrui Yang, Xiawu Zheng, Ke Li, Xing Sun, et al. Mme: A comprehensive evaluation benchmark for multimodal large language models. *arXiv preprint arXiv:2306.13394*, 2023. 3
- [17] Jiahui Gao, Renjie Pi, Jipeng Zhang, Jiacheng Ye, Wan-jun Zhong, Yufei Wang, Lanqing Hong, Jianhua Han, Hang Xu, Zhenguo Li, et al. G-llava: Solving geometric problem with multi-modal large language model. In *The Thirteenth International Conference on Learning Representations*, 2025. 1, 2, 3, 4
- [18] Juraj Gottweis, Wei-Hung Weng, Alexander Daryin, Tao Tu, Anil Palepu, Petar Sirkovic, Artiom Myaskovsky, Felix Weissenberger, Keran Rong, Ryutaro Tanno, et al. Towards an ai co-scientist. *arXiv preprint arXiv:2502.18864*, 2025. 3
- [19] Yihan Hao, Mingliang Zhang, Fei Yin, and Lin-Lin Huang. Pgdp5k: A diagram parsing dataset for plane geometry problems. In *2022 26th International Conference on Pattern Recognition (ICPR)*, pages 1763–1769. IEEE, 2022. 1, 3
- [20] Chaoqun He, Renjie Luo, Yuzhuo Bai, Shengding Hu, Zhen Leng Thai, Junhao Shen, Jinyi Hu, Xu Han, Yujie Huang, Yuxiang Zhang, et al. Olympiadbench: A challenging benchmark for promoting agi with olympiad-level bilingual multimodal scientific problems. *arXiv preprint arXiv:2402.14008*, 2024. 2, 3
- [21] Dongzhi Jiang, Renrui Zhang, Ziyu Guo, Yanwei Li, Yu Qi, Xinyan Chen, Lihui Wang, Jianhan Jin, Claire Guo, Shen Yan, et al. Mme-cot: Benchmarking chain-of-thought in large multimodal models for reasoning quality, robustness, and efficiency. *arXiv preprint arXiv:2502.09621*, 2025. 3
- [22] Jacques Leonardi, Jan-Hendrik Müller, Sascha Stöpelkamp, Sven-Thomas Graupner, Jens Schade, Malin Stoldt, Tomas Hagelberg, Jonas Malmryd, Lillian Hansen, Petter Arnesen, et al. Geosence report on impact assessment and evaluation. Technical report, CLOSER, 2024. 2
- [23] Junnan Li, Dongxu Li, Silvio Savarese, and Steven Hoi. Blip-2: Bootstrapping language-image pre-training with frozen image encoders and large language models. In *International conference on machine learning*, pages 19730–19742. PMLR, 2023. 3
- [24] Zhenwen Liang, Tianyu Yang, Jipeng Zhang, and Xiangliang Zhang. Unimath: A foundational and multimodal mathematical reasoner. In *Proceedings of the 2023 Conference on Empirical Methods in Natural Language Processing*, pages 7126–7133, 2023. 1
- [25] Haotian Liu, Chunyuan Li, Qingyang Wu, and Yong Jae Lee. Visual instruction tuning. *Advances in neural information processing systems*, 36, 2024. 3, 8
- [26] Haoyu Lu, Wen Liu, Bo Zhang, Bingxuan Wang, Kai Dong, Bo Liu, Jingxiang Sun, Tongzheng Ren, Zhuoshu Li, Hao Yang, et al. Deepseek-vl: towards real-world vision-language understanding. *arXiv preprint*

- arXiv:2403.05525*, 2024. 1
- [27] Pan Lu, Hritik Bansal, Tony Xia, Jiacheng Liu, Chunyuan Li, Hannaneh Hajishirzi, Hao Cheng, Kai-Wei Chang, Michel Galley, and Jianfeng Gao. Mathvista: Evaluating mathematical reasoning of foundation models in visual contexts. In *The Twelfth International Conference on Learning Representations*, 2024. 1, 2, 3
- [28] Pan Lu, Ran Gong, Shibiao Jiang, Liang Qiu, Siyuan Huang, Xiaodan Liang, and Song-Chun Zhu. Intergps: Interpretable geometry problem solving with formal language and symbolic reasoning. *arXiv preprint arXiv:2105.04165*, 2021. 1, 2, 3
- [29] OpenAI. Gpt-4v. <https://openai.com/index/gpt-4v-system-card/>, 2023. 1
- [30] OpenAI. Hello gpt-4o. <https://openai.com/index/hello-gpt-4o/>, 2024. 1, 8, 9
- [31] OpenAI. OpenAI o3 and o4-mini System Card. Technical report, OpenAI, April 2025. 8, 9
- [32] Long Ouyang, Jeffrey Wu, Xu Jiang, Diogo Almeida, Carroll Wainwright, Pamela Mishkin, Chong Zhang, Sandhini Agarwal, Katarina Slama, Alex Ray, et al. Training language models to follow instructions with human feedback. *Advances in neural information processing systems*, 35:27730–27744, 2022. 3
- [33] Tianshuo Peng, Mingsheng Li, Hongbin Zhou, Renqiu Xia, Renrui Zhang, Lei Bai, Song Mao, Bin Wang, Conghui He, Aojun Zhou, et al. Chimera: Improving generalist model with domain-specific experts. *arXiv preprint arXiv:2412.05983*, 2024. 1
- [34] Machel Reid, Nikolay Savinov, Denis Teplyashin, Dmitry Lepikhin, Timothy Lillicrap, Jean-baptiste Alayrac, Radu Soricut, Angeliki Lazaridou, Orhan Firat, Julian Schrittwieser, et al. Gemini 1.5: Unlocking multimodal understanding across millions of tokens of context. *arXiv preprint arXiv:2403.05530*, 2024. 3
- [35] Wenhao Shi, Zhiqiang Hu, Yi Bin, Junhua Liu, Yang Yang, See-Kiong Ng, Lidong Bing, and Roy Ka-Wei Lee. Math-llava: Bootstrapping mathematical reasoning for multimodal large language models. *arXiv preprint arXiv:2406.17294*, 2024. 1
- [36] Vladimir Sicca, Tianxiang Xia, Mathis Fédérico, Philip John Gorinski, Simon Frieder, and Shangling Jui. Newclid: A user-friendly replacement for alphageometry. *arXiv preprint arXiv:2411.11938*, 2024. 3
- [37] InternLM Team. Internlm: A multilingual language model with progressively enhanced capabilities, 2023. 3
- [38] NovelSeek Team, Bo Zhang, Shiyang Feng, Xiangchao Yan, Jiakang Yuan, Zhiyin Yu, Xiaohan He, Songtao Huang, Shaowei Hou, Zheng Nie, et al. Novelseek: When agent becomes the scientist—building closed-loop system from hypothesis to verification. *arXiv preprint arXiv:2505.16938*, 2025. 3
- [39] Hugo Touvron, Thibaut Lavril, Gautier Izacard, Xavier Martinet, Marie-Anne Lachaux, Timothée Lacroix, Baptiste Rozière, Naman Goyal, Eric Hambro, Faisal Azhar, et al. Llama: Open and efficient foundation language models. *arXiv preprint arXiv:2302.13971*, 2023. 3
- [40] Hugo Touvron, Louis Martin, Kevin Stone, Peter Albert, Amjad Almahairi, Yasmine Babaei, Nikolay Bashlykov, Soumya Batra, Prajwal Bhargava, Shruti Bhosale, et al. Llama 2: Open foundation and fine-tuned chat models. *arXiv preprint arXiv:2307.09288*, 2023. 3
- [41] Trieu Trinh, Yuhuai Wu, Quoc Le, He He, and Thang Luong. Solving olympiad geometry without human demonstrations. *Nature*, 2024. 1, 3
- [42] Peng Wang, Shuai Bai, Sinan Tan, Shijie Wang, Zhihao Fan, Jinze Bai, Keqin Chen, Xuejing Liu, Jialin Wang, Wenbin Ge, Yang Fan, Kai Dang, Mengfei Du, Xuancheng Ren, Rui Men, Dayiheng Liu, Chang Zhou, Jingren Zhou, and Junyang Lin. Qwen2-vl: Enhancing vision-language model’s perception of the world at any resolution. *ArXiv*, abs/2409.12191, 2024. 8
- [43] Zhiyu Wu, Xiaokang Chen, Zizheng Pan, Xingchao Liu, Wen Liu, Damai Dai, Huazuo Gao, Yiyang Ma, Chengyue Wu, Bingxuan Wang, Zhenda Xie, Yu Wu, Kai Hu, Jiawei Wang, Yaofeng Sun, Yukun Li, Yishi Piao, Kang Guan, Aixin Liu, Xin Xie, Yuxiang You, Kai Dong, Xingkai Yu, Haowei Zhang, Liang Zhao, Yisong Wang, and Chong Ruan. Deepseek-vl2: Mixture-of-experts vision-language models for advanced multimodal understanding, 2024. 1
- [44] Renqiu Xia, Mingsheng Li, Hancheng Ye, Wenjie Wu, Hongbin Zhou, Jiakang Yuan, Tianshuo Peng, Xinyu Cai, Xiangchao Yan, Bin Wang, Conghui He, Botian Shi, Tao Chen, Junchi Yan, and Bo Zhang. Geox: Geometric problem solving through unified formalized vision-language pre-training. In *The Thirteenth International Conference on Learning Representations*, 2025. 1, 3
- [45] Renqiu Xia, Song Mao, Xiangchao Yan, Hongbin Zhou, Bo Zhang, Haoyang Peng, Jiahao Pi, Daocheng Fu, Wenjie Wu, Hancheng Ye, et al. Docgenome: An open large-scale scientific document benchmark for training and testing multi-modal large language models. *arXiv preprint arXiv:2406.11633*, 2024. 3
- [46] Renqiu Xia, Bo Zhang, Haoyang Peng, Ning Liao, Peng Ye, Botian Shi, Junchi Yan, and Yu Qiao. Structchart: Perception, structuring, reasoning for visual chart understanding. *arXiv preprint arXiv:2309.11268*, 2023. 3
- [47] Ling Yang, Zhaochen Yu, Bin Cui, and Mengdi Wang. Reasonflux: Hierarchical llm reasoning via scaling thought templates. *arXiv preprint arXiv:2502.06772*, 2025. 6
- [48] Yixin Ye, Zhen Huang, Yang Xiao, Ethan Chern, Shijie Xia, and Pengfei Liu. Limo: Less is more for reasoning. *arXiv preprint arXiv:2502.03387*, 2025. 6
- [49] Chi Zhang, Jiajun Song, Siyu Li, Yitao Liang, Yuxi Ma, Wei Wang, Yixin Zhu, and Song-Chun Zhu. Proposing and solving olympiad geometry with guided tree search. *ArXiv*, abs/2412.10673, 2024. 1
- [50] Jiaxin Zhang, Zhongzhi Li, Mingliang Zhang, Fei Yin, Chenglin Liu, and Yashar Moshfeghi. Geoeval: benchmark for evaluating llms and multi-modal models on geometry problem-solving. *arXiv preprint arXiv:2402.10104*, 2024. 2
- [51] Ming-Liang Zhang, Fei Yin, and Cheng-Lin Liu. A multi-modal neural geometric solver with textual clauses parsed from diagram. *arXiv preprint arXiv:2302.11097*, 2023. 1, 2, 3
- [52] Renrui Zhang, Dongzhi Jiang, Yichi Zhang, Haokun Lin, Ziyu Guo, Pengshuo Qiu, Aojun Zhou, Pan Lu,

Kai-Wei Chang, Yu Qiao, et al. Mathverse: Does your multi-modal llm truly see the diagrams in visual math problems? In *European Conference on Computer Vision*, pages 169–186. Springer, 2024. [2](#)

- [53] Renrui Zhang, Xinyu Wei, Dongzhi Jiang, Yichi Zhang, Ziyu Guo, Chengzhuo Tong, Jiaming Liu, Aojun Zhou, Bin Wei, Shanghang Zhang, et al. Mavis: Mathematical visual instruction tuning. *arXiv preprint arXiv:2407.08739*, 2024. [1](#), [2](#), [3](#), [4](#)

- [54] Zhongyue Zhang, Zijie Qiu, Yingcheng Wu, Shuya Li, Dingyan Wang, Zhuomin Zhou, Duo An, Yuhan Chen, Yu Li, Yongbo Wang, et al. Origene: A self-evolving virtual disease biologist automating therapeutic target discovery. *bioRxiv*, pages 2025–06, 2025. [3](#)